

11-21-2019

BODIPY-Caged Photoactivated Inhibitors of Cathepsin B Flip the Light Switch on Cancer Cell Apoptosis

Nicholas P. Toupin
Wayne State University

Karan Arora
Wayne State University

Pradeep Shrestha
Iowa State University, pradeeps@iastate.edu

Julie A. Peterson
Iowa State University, japete@iastate.edu

Logan J. Fischer
Iowa State University, lofisch@iastate.edu

See next page for additional authors

Follow this and additional works at: https://lib.dr.iastate.edu/chem_pubs

 Part of the [Medicinal-Pharmaceutical Chemistry Commons](#)

The complete bibliographic information for this item can be found at https://lib.dr.iastate.edu/chem_pubs/1188. For information on how to cite this item, please visit <http://lib.dr.iastate.edu/howtocite.html>.

This Article is brought to you for free and open access by the Chemistry at Iowa State University Digital Repository. It has been accepted for inclusion in Chemistry Publications by an authorized administrator of Iowa State University Digital Repository. For more information, please contact digirep@iastate.edu.

BODIPY-Caged Photoactivated Inhibitors of Cathepsin B Flip the Light Switch on Cancer Cell Apoptosis

Abstract

Acquired resistance to apoptotic agents is a long-standing challenge in cancer treatment. Cathepsin B (CTSB) is an enzyme which, among many essential functions, promotes apoptosis during cellular stress through regulation of intracellular proteolytic networks on the minute timescale. Recent data indicate that CTSB inhibition may be a promising method to steer cells away from apoptotic death towards necrosis, a mechanism of cell death that can overcome resistance to apoptotic agents, stimulate an immune response and promote anti-tumor immunity. Unfortunately, rapid and selective intracellular inactivation of CTSB has not been possible. However, here we report on the synthesis and characterization of photochemical and biological properties of BODIPY-caged inhibitors of CTSB that are cell permeable, highly selective and activated rapidly upon exposure to visible light. Intriguingly, these compounds display tunable photophysical and biological properties based on substituents bound directly to boron. Me2BODIPY-caged compound **8** displays the dual-action capability of light-accelerated CTSB inhibition and singlet oxygen production from a singular molecular entity. The dual-action capacity of **8** leads to a rapid necrotic response in MDA-MB-231 triple negative breast cancer cells with high phototherapeutic indexes (>30) and selectivity vs. non-cancerous cells that neither CTSB inhibition nor photosensitization gives alone. Our work confirms that singlet oxygen production and CTSB inactivation is highly synergistic and a promising method for killing cancer cells. Furthermore, our ability to trigger intracellular inactivation of CTSB with light will provide researchers with a powerful photochemical tool for probing biochemical processes on short timescales.

Disciplines

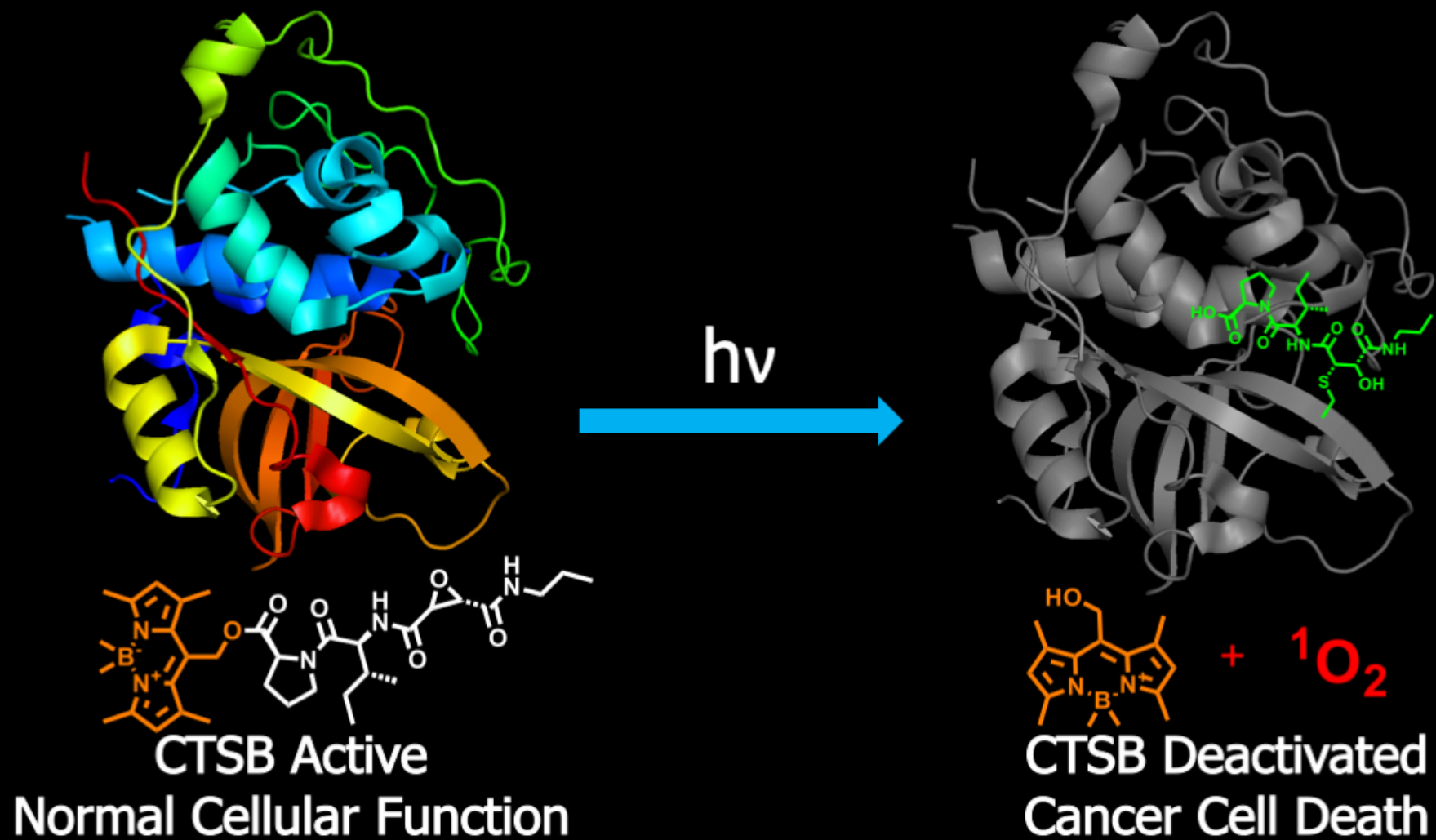
Medicinal-Pharmaceutical Chemistry

Comments

This document is the unedited Author's version of a Submitted Work that was subsequently accepted for publication in *ACS Chemical Biology*, copyright © American Chemical Society after peer review. To access the final edited and published work see DOI: [10.1021/acscchembio.9b00711](https://doi.org/10.1021/acscchembio.9b00711). Posted with permission.

Authors

Nicholas P. Toupin, Karan Arora, Pradeep Shrestha, Julie A. Peterson, Logan J. Fischer, Erandi Rajagurubandara, Izabela Podgorski, Arthur H. Winter, and Jeremy J. Kodanko

1
2
3
440
41
42
43
44
45
46
47

BODIPY-Caged Photoactivated Inhibitors of Cathepsin B Flip the Light Switch on Cancer Cell Apoptosis

Nicholas P. Toupin,¹ Karan Arora,¹ Pradeep Shrestha,² Julie A. Peterson,² Logan J. Fischer,² Erandi Rajagurubandara,⁴ Izabela Podgorski,^{3,4} Arthur H. Winter,^{*2} and Jeremy J. Kodanko^{*1,3}

¹ Department of Chemistry, Wayne State University, 5101 Cass Ave, Detroit, MI 48202

² Department of Chemistry, Iowa State University, Ames, Iowa 50014, United States

³ Barbara Ann Karmanos Cancer Institute, Detroit, Michigan 48201

⁴ Department of Pharmacology, School of Medicine, Wayne State University, Detroit, Michigan 48201, United States

Email: jkodanko@chem.wayne.edu, winter@iastate.edu

Abstract. Acquired resistance to apoptotic agents is a long-standing challenge in cancer treatment. Cathepsin B (CTSB) is an enzyme which, among many essential functions, promotes apoptosis during cellular stress through regulation of intracellular proteolytic networks on the minute timescale. Recent data indicate that CTSB inhibition may be a promising method to steer cells away from apoptotic death towards necrosis, a mechanism of cell death that can overcome resistance to apoptotic agents, stimulate an immune response and promote anti-tumor immunity. Unfortunately, rapid and selective intracellular inactivation of CTSB has not been possible. However, here we report on the synthesis and characterization of photochemical and biological properties of BODIPY-caged inhibitors of CTSB that are cell permeable, highly selective and activated rapidly upon exposure to visible light. Intriguingly, these compounds display tunable photophysical and biological properties based on substituents bound directly to boron. Me₂BODIPY-caged compound **8** displays the dual-action capability of light-accelerated CTSB inhibition and singlet oxygen production from a singular molecular

1 entity. The dual-action capacity of **8** leads to a rapid necrotic response in MDA-MB-231 triple negative breast
2 cancer cells with high phototherapeutic indexes (>30) and selectivity vs. non-cancerous cells that neither CTSB
3 inhibition nor photosensitization gives alone. Our work confirms that singlet oxygen production and CTSB
4 inhibition nor photosensitization gives alone. Our work confirms that singlet oxygen production and CTSB
5 inactivation is highly synergistic and a promising method for killing cancer cells. Furthermore, this ability to
6 trigger intracellular inactivation of CTSB with light provides researchers with a powerful photochemical tool
7 for probing biochemical processes on short timescales.
8
9

10
11
12
13
14
15
16 **Introduction.** The cysteine protease cathepsin B (CTSB) is a crucial enzyme in biology with a broad scope of
17 functions that include degradation of proteins and organelles, antigen presentation¹ and execution of cell death
18 pathways.² Aberrant CTSB activity is associated with many human disease states, including obesity³ diabetes,⁴
19 non-alcoholic fatty liver disease,⁵ pancreatitis⁶ and cancer.^{7,8} In order to understand the role of CTSB in biology
20 and also target human diseases, small molecule inhibitors of this protease have been aggressively pursued.⁹⁻¹¹
21
22
23
24
25
26
27

28 CTSB inhibitors have served as indispensable chemical tools; some inhibitors, either alone or in
29 combination with other agents, have shown promise as potential therapeutics in cell and animal models of
30 human diseases.^{8, 12, 13} This class of small molecules includes reversible and irreversible inhibitors, where
31 most contain chemical “warheads” that target the active site cysteine through covalent modification. To date,
32 irreversible CTSB inhibitors based on epoxides, namely CA-074 (**1**)¹⁴ and its methyl ester prodrug form CA-
33 074-Me (**2**),¹⁵ have been the most widely used (Figure 1). CA-074 contains a carboxylic acid and is not cell
34 permeable, whereas methyl ester **2** is. Compounds **1** and **2** are routinely used by researchers working *in vitro*
35 to target extra- and intracellular activity of CTSB, respectively.¹⁶⁻²¹ Although it is widely assumed that **2**
36 undergoes rapid conversion to **1** in cells, careful studies have established that **2** is not a selective inhibitor of
37 intracellular CTSB activity because it inactivates other cysteine proteases,^{22, 23} likely due to the slow
38 hydrolysis of **2** by intracellular esterases and the poor selectivity of **2** for CTSB inactivation vs. other cysteine
39 cathepsins.²⁴ Although some potent and selective CTSB inhibitors have been developed,²⁵⁻²⁷ a major
40
41
42
43
44
45
46
47
48
49
50
51
52
53
54
55
56
57
58
59
60

drawback to the suite of small molecule tools currently available is that there is no method to rapidly and selectively inactivate CTSB inside cells.

CTSB is a prognostic biomarker for many types of cancer^{28, 29} and its intra- and extracellular activity is intimately linked to most steps of tumor progression including invasion, migration, metastasis, and angiogenesis.³⁰⁻³² Given its broad range of functions inside and outside the cell, targeting intra- and extracellular proteolysis by CTSB may be necessary for effective cancer treatment. Furthermore, CTSB inhibition may need to be combined with other treatment modalities, such as chemotherapy, radiation or photodynamic therapy, to achieve successful outcomes.^{9, 33, 34}

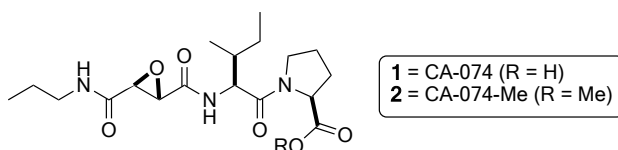


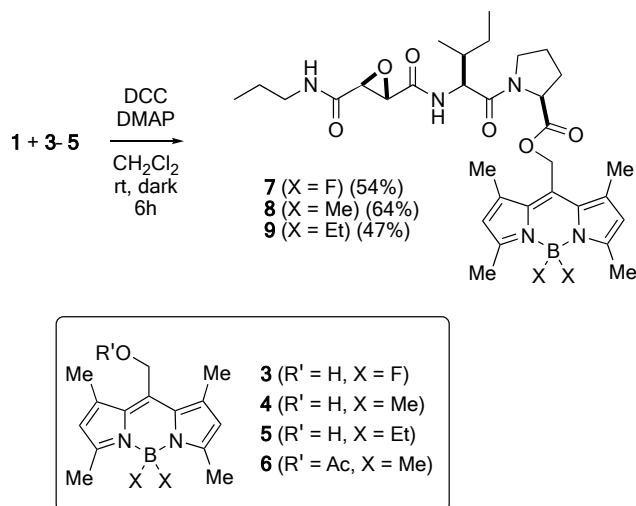
Figure 1. Structures of epoxysuccinyl inhibitors CA-074 (**1**) and the methyl ester prodrug CA-074-Me (**2**).

Through positive selection of resistant cells, pharmacological agents that induce apoptosis can lead to rapid resistance and poor therapeutic outcomes during cancer treatment.³⁵ In an effort to avoid these issues, researchers have renewed interest in agents that cause death by mechanisms other than apoptosis.³⁶ Necrosis and its programmed counterpart necroptosis have garnered recent attention as promising strategies to overcome resistance to clinical apoptotic agents³⁷ stimulate the immune system³⁸ and build anti-tumor immunity.³⁹ Recent data confirm that CTSB plays a major role in controlling the balance between apoptotic and necrotic death in cells under stress conditions. Importantly, active CTSB functions as an emergency brake to steer cells under stress away from necrosis towards apoptotic death.^{40, 41} CTSB carries out this function through rapid regulation of proteolytic networks on the minute timescale by inhibiting degradation of the pro-apoptotic proteins bid and bax and accelerating cleavage of the anti-apoptotic protein bcl-xl. Therefore, combining rapid, intracellular CTSB inhibition with another mechanism that induces cell stress has great potential to steer cells away from apoptotic death towards necrosis.

1 Here we report the synthesis, photochemical and biological characterization of BODIPY-caged CTSB
2 inhibitors that are cell permeable and are activated rapidly with visible light. This study reports a new class of
3 highly tunable chemical tools for investigating the role of intracellular CTSB activity. Our lead compound
4 inactivates CTSB with >700-fold kinetic control under light vs. dark conditions and >200-fold selectivity over
5 inactivation of the related cysteine protease cathepsin L (CTSL). In addition to control over CTSB inactivation
6 through rapid photochemical uncaging, we demonstrate that the released BODIPY dye can act as a
7 photosensitizer to generate singlet oxygen ($^1\text{O}_2$). Importantly, efficiencies of photorelease and
8 photosensitization are highly tunable based on substituents bound directly to boron, which leads to control over
9 the levels of cell death in breast cancer cells, with high phototherapeutic indexes and selectivity over normal
10 breast epithelial cells. Collectively, our data show that synergistic and rapid CTSB inactivation and oxidative
11 stress steer cancer cells towards necrotic death, a response that neither CTSB inhibition nor photosensitization
12 gives alone.

13 **Results and Discussion**

14 To develop photocaged CTSB inhibitors, we combined the highly potent and selective, but cell
15 impermeable, inhibitor CA-074 (**1**)¹⁴ with BODIPY-based photocaging groups⁴²⁻⁴⁴ (Scheme 1A). BODIPY
16 photocages are attractive because they release carboxylates when irradiated over a broad range of the visible
17 spectrum which provides an advantage over most organic photocaging groups that require UV light for
18 cleavage. Caging of the free carboxylic acid motif in **1** with BODIPY was expected to facilitate membrane
19 permeability and slow inactivation by blocking key interactions of the free acid with the CTSB active site,
20 much like the known methyl ester derivative CA-074-OMe (**2**).¹⁵ However, unlike **2**, which is not selective
21 amongst other cysteine cathepsins and undergoes slow conversion to **1** by intracellular esterases,^{22, 23} photolysis
22 of a BODIPY-caged inhibitor was expected to facilitate rapid intracellular release of the potent and selective
23 inhibitor **1**.



21
22
23
24
25
26
27
28
29
30
31
32

Scheme 1. Synthesis of BODIPY-caged CA-074 inhibitors **7–9**

Three BODIPY-caged CA-074 derivatives were prepared through carbodiimide coupling reactions between **1** and the known BODIPY alcohols **3–5** to furnish caged inhibitors **7–9** (Scheme 1). Compounds **7–9** were characterized by ^1H and ^{13}C NMR and electronic absorbance spectroscopies and high-resolution mass spectrometry. BODIPY-caged derivatives **7–9** all absorb strongly from ~ 400 – 550 nm, with λ_{max} values ranging from 515–522 nm ($\epsilon = 55,300$ – $71,000 \text{ M}^{-1}\text{cm}^{-1}$, Figure S40).

33
34
35
36
37
38
39
40
41
42
43
44
45
46
47
48
49
50
51
52
53
54
55
56
57
58
59
60

Photochemical investigations with **7–9** indicated that the efficiency of uncaging and photoactivated enzyme inhibition are highly tunable based on the nature of the boron substituent X (Scheme 1B). Photodecomposition quantum yields were determined in methanol upon irradiation with a Nd:YAG laser ($\lambda_{\text{irr}} = 532$ nm) by following decomposition of **7–9** by electronic absorption spectroscopy. Compound **8** (X = Me) displayed a photodecomposition quantum yield of $2.46 \pm 0.19\%$. Photolysis of **8** with blue light ($\lambda_{\text{irr}} = 460$ – 470 nm) generated CA-074 (**1**) and alcohol **4**, as judged by LCMS analysis. Interestingly, a photodecomposition quantum yield of $0.56 \pm 0.02\%$ was observed for the related Et derivative **9**, which is almost 5 times less than the yield observed for **8**. The photodecomposition quantum yield observed for **7** (X = F) was significantly lower ($0.19 \pm 0.02\%$), which is almost 13 times smaller than the yield observed for **8**. Collectively, these data are similar to previous observations for release of acetate from Me, Et and F BODIPY caging groups (eg. **6**),

1 confirming that the efficiency of uncaging is tunable based on the substituent X, and that photolysis of
2 BODIPY-protected esters leads to carboxylic acid and BODIPY-derived alcohol byproducts.⁴⁵
3
4

5
6
7 To further assess the photodissociative action of **7–9** we evaluated the ability of these compounds to
8 inactivate purified CTSB before and after irradiation with visible light. Solutions of **7–9** (100 nM) in CTSB
9 activity assay buffer were irradiated ($\lambda_{\text{irr}} = 395\text{--}750$ nm) for 1–30 min. Purified human CTSB was added and
10 enzyme activities were determined at five time intervals of irradiation using the fluorogenic substrate Z-Arg-
11 Arg-AMC. Compound **8** shows 100% activity at $t = 0$, but after only 5 min of irradiation CTSB activity drops
12 to $< 1\%$. In contrast, CTSB is still active with **7** and **9** after 10 and 30 min of irradiation, respectively (Figure
13 S15-S17). These data show that the rate of photochemical activation of the irreversible inhibitor is highly
14 tunable based on the boron substituent X and establish compound **8** as a lead inhibitor
15
16
17
18
19
20
21
22
23
24
25

26 In order to gain a more quantitative assessment of the levels of photochemical inhibitor activation, progress
27 curve analysis was used to measure levels of rate acceleration for CTSB inactivation under light vs. dark
28 conditions (Table 1). CTSB activity was monitored over time in the presence of the fluorogenic substrate Z-
29 Arg-Arg-AMC and varied amounts of inhibitor. Data were fit to a two-step model for irreversible inactivation
30 (Figures S13–14).^{45, 46} The equilibrium constant for reversible association of the inhibitors with CTSB (K_i) and
31 the rate constant for irreversible inactivation due to epoxide opening (k_{inact}) were determined, where k_{inact}/K_i
32 represents the overall second order rate constant for enzyme inactivation. The second order rate constant for **1**
33 is in good agreement with literature values,⁴⁶ and was the same within error under dark and light conditions
34 ($\lambda_{\text{irr}} = 395\text{--}750$ nm), indicating that light alone does not affect CTSB activity (Entry 1). In contrast, **8** inactivates
35 CTSB at a rate of $220 \pm 20 \times 10^3 \text{ M}^{-1} \text{ s}^{-1}$ with light irradiation, which is 760 times faster than the rate observed
36 in the dark (Entry 4). This large difference is due to weaker equilibrium binding of **8** with CTSB in the dark
37 ($K_i = 320 \pm 30 \text{ } \mu\text{M}$) vs. in the light ($K_i = 0.51 \pm 0.09 \text{ } \mu\text{M}$), rather than changes in k_{inact} , which were the same
38 within error under light and dark conditions (Entry 4). The light to dark ratio for **8** is in good agreement with
39
40
41
42
43
44
45
46
47
48
49
50
51
52
53
54
55
56
57
58
59
60

relative rates of inactivation by acid **1** vs. ester **2**, which differ by roughly three orders of magnitude.⁴⁷ Compound **8** inactivated CTSB ~50% more rapidly than **1** under light conditions, which may be due to inactivation of CTSB by reactive oxygen species (ROS) generated after release of **1** (*vide infra*). However, the control compound **6**, which releases acetate and **4** upon photolysis, was not a potent inhibitor under light or dark conditions, indicating that the BODIPY photocaging group and its photochemical products were not dominant in the inactivation of CTSB by **8** (Entry 2). Data for **9** in the dark (Entry 5) were within error of **8**, which were both about 10 times smaller than the second order rate constant obtained for **7** (Entry 3), indicating that the nature of the boron substituent X does control inactivation of CTSB in the dark. Data for **7** and **9** in the light were not collected, due to partial release of **1** from both compounds after 15 min of irradiation. Cathepsin L (CTSL) inactivation experiments indicated that **8** is 220 times more selective for CTSB over CTSL under light conditions (Table S2), similar to **1**.⁴⁶ Compound **8** displayed rate constants for inactivation of CTSL of $1.0 \pm 0.9 \times 10^3 \text{ M}^{-1} \text{ s}^{-1}$ and $10.0 \pm 3.0 \text{ M}^{-1} \text{ s}^{-1}$ in the light and dark, respectively.

Table 1. Irreversible inhibition of CTSB by **1**, **6–9** [a]

Entry	Compounds	Light k_{inact} (s^{-1})	Light K_i (μM)	Light		Dark		Light/Dark Ratio ^[e]
				k_{inact}/K_i ($\times 10^3 \text{ M}^{-1}\text{s}^{-1}$)	Dark k_{inact} (s^{-1})	Dark K_i (μM)	k_{inact}/K_i ($\times 10^3 \text{ M}^{-1}\text{s}^{-1}$)	
1	1	$1.1 \pm 0.1 \times 10^{-1}$	$7.8 \pm 0.3 \times 10^{-1}$	140 ± 10	$1.0 \pm 0.1 \times 10^{-1}$	$8.1 \pm 0.3 \times 10^{-1}$	130 ± 10	1.1
2	6	$1.7 \pm 1.0 \times 10^{-2}$	$1.8 \pm 0.4 \times 10^3$	0.0010 ± 0.0003	$1.7 \pm 0.8 \times 10^{-2}$	$1.4 \pm 0.5 \times 10^3$	0.0012 ± 0.0002	0.83
3	7	nd ^b	nd ^b	nd ^b	$1.9 \pm 0.1 \times 10^{-1}$	$9.4 \pm 0.3 \times 10^1$	2.1 ± 0.1	-
4	8	$1.1 \pm 0.1 \times 10^{-1}$	$5.1 \pm 0.9 \times 10^{-1}$	220 ± 20	$8.9 \pm 0.1 \times 10^{-2}$	$3.2 \pm 0.3 \times 10^2$	0.29 ± 0.03	760
5	9	nd ^b	nd ^b	nd ^b	$8.9 \pm 0.1 \times 10^{-2}$	$3.5 \pm 0.2 \times 10^2$	0.26 ± 0.01	-

1 [a] Second-order μs for enzyme inactivation obtained from progress curve analysis with CTSB (4 nM), Z-Arg-Arg-AMC (100 μM), **1** or **6–9** (5 nM – 50 μM) in 0.4
2 M acetate buffer, pH 5.5, <1% DMSO, 4 mM EDTA, 0.01% Triton X-100, DTT = 8 mM at 25 °C under dark or light conditions ($t_{\text{irr}} = 15$ min, $\lambda_{\text{irr}} = 395\text{--}750$ nm).
3 [b] Not determined due to partial release of **1** after 15 min irradiation. [c] Ratio of light k_{inact}/K_i to dark k_{inact}/K_i
4
5

6
7 After confirming that **8** is a highly potent and selective inactivator of CTSB under light conditions, we
8 sought to determine its ability to inactivate CTSB *in cellulo*. Triple-negative MDA-MB-231 breast cancer cells
9 were treated with **8** (2.5 μM) and left in the dark or irradiated for 15 min with a LED panel designed for 96
10 well plates (see S1, $\lambda_{\text{irr}} = 460\text{--}470$ nm). Lysates were collected after 4 h, and activity of CTSB was determined.
11 Data confirmed that intracellular CTSB was targeted with **8** and that the enzyme inactivated fully under light
12 and dark conditions at 4 h in cells treated with **8** relative to vehicle control (Table S3). Even though a difference
13 between CTSB activity under light vs. dark conditions was not observed after 4 h, visual inspection of cells
14 treated with **8** and light indicated substantial rounding, an increase in granularity and notable cell detachment
15 compared with treatment with **8** in the dark, suggesting that the combination of **8** and light was causing an
16 immediate toxic effect in the MDA-MB-231 cells that was consistent with necrosis (*vide infra*) and warranted
17 further investigation.
18
19
20
21
22
23
24
25
26
27
28
29
30
31
32

33 EC_{50} determinations were carried out with MDA-MB-231 cells via the 3-(4,5-Dimethyl-2-thiazolyl)-2,5-
34 diphenyl-2H-tetrazolium bromide (MTT) assay to quantify cell toxicities. First, the irradiation protocol was
35 optimized. After only 1 min of irradiation ($\lambda_{\text{irr}} = 460\text{--}470$ nm), viability after 4 h was reduced to ~40% vs.
36 DMSO vehicle upon treatment with **8** (10 μM). After 5 min of irradiation, viabilities were reduced to <10%
37 and were not reduced further with longer irradiation times. However, 15 min of irradiation was used in all
38 subsequent experiments to maximize release of **1** from **8** at higher concentrations. EC_{50} values were obtained
39 for **2** and **6–8** at 4 and 72 h under light ($\lambda_{\text{irr}} = 460\text{--}470$ nm, $t = 15$ min) or in constant darkness (Table 2). At 4
40 h, Me_2BODIPY caged inhibitor **8** exhibits an EC_{50} value of 2.5 μM post irradiation ($\lambda_{\text{irr}} = 460\text{--}470$ nm, $t = 15$
41 min) vs. >100 μM in the dark, giving a phototherapeutic index (PI) of > 40 (Entry 6). Interestingly, **2** (Entry 1)
42 or **6** (Entry 3) alone or in equimolar combination (Entry 4) showed no toxicity at 50 μM under light or dark
43
44
45
46
47
48
49
50
51
52
53
54
55
56
57
58
59
60

conditions at 4 h. These data are consistent with **8** being resistant to rapid esterase cleavage in cells, because the combination of **2** and **6** would be expected to give the same products as **8** (**1** and **4**) if rapid esterase cleavage were occurring. EC₅₀ values for **7** and **9** were also >100 μM (Entries 5 and 8), which correlates the rate of photochemical release of **1** from **7–9** with cell toxicity; only **8**, which provides rapid and efficient release of **1** causes cell death in the low μM-nM range. At 72 h, **8** gave an EC₅₀ of 780 nM in the light versus 24 μM in the dark, with PI = 30 (Entry 6). Toxicity of **8** after 72 h in the dark was similar to **2** in the dark and light (Entry 1), which is consistent with slow release of **1**, likely from esterases, causing some level of growth arrest over long time periods. EC₅₀ values were also determined for **2** (Entry 2) and **8** (Entry 7) using the normal human epithelial breast cells (MCF-10A). At 4 and 72 h, EC₅₀ values for **8** in MCF-10A cells were 10.3 μM and 3.5 μM respectively, indicating that **8** displayed a 4-fold higher selectivity towards cancer cells vs. normal epithelial cells at both time points with light irradiation.

Table 2. EC₅₀ values (μM) for **2**, **6–9** against MDA-MB-231^[a] and MCF-10A^[b] cells at 4 and 72 h^[c]

Entry	Compound	Light (4h)	Dark (4h)	PI ^[d] (4h)	Light (72h)	Dark (72h)	PI ^[d] (72h)
1	2 ^[a]	>100	>100	-	33 ± 8.7	21 ± 5.1	0.6
2	2 ^[b]	>100	>100	-	49 ± 0.5	49 ± 5.5	1.0
3	6 ^[a]	>50	>50	-	>50	>50	-
4	2 + 6 ^{[a],[e]}	>50	>50	-	nd ^[f]	nd ^[f]	-
5	7 ^[a]	>50	>50	-	>50	>50	-
6	8 ^[a]	2.5 ± 0.22	>100	>40	0.78 ± 0.14	24 ± 3.3	30
7	8 ^[b]	10.3 ± 2.0	>100	>9	3.5 ± 1.3	27 ± 11.5	7.7
8	9 ^[a]	>50	>50	-	>50	>50	-

[a,b] Cells were treated with compound **2**, **6–9** for 5 min, then irradiated (t = 15 min, λ_{irr} = 460–470 nm) or left in the dark. [c] Cell viabilities were determined by MTT after 4 and 72 h. Data are average of three independent experiments using quadruplicate wells, errors are standard deviations. [d] PI = phototherapeutic index = ratio dark EC₅₀/light EC₅₀. [e] Cells were treated simultaneously with equimolar amounts of **2** and **6**.

Data from toxicity studies indicated that the combination of **8** and light were required to achieve cell death at low concentrations. BODIPY dyes have previously shown excellent photosensitization capacities.⁴⁸ To investigate the role of ROS, cells were pretreated with ROS scavengers NaN₃, which quenches ¹O₂, histidine (50 mM), which quenches hydroxyl radical and ¹O₂ to a lesser extent than NaN₃,⁴⁹ and mannitol (50 mM) which quenches hydroxyl radical, before treatment with **8** (10 μM) and light (λ_{irr} = 460–470 nm, t = 15 min) (Figure 2). Only NaN₃ provided a high level of rescue, implicating ¹O₂ in the cell death mechanism. Further investigation showed that NaN₃ (10–100 mM) provided a dose dependent rescue of cells treated with **8** (10 μM) and light but did not rescue cells fully from death at the highest concentration tested, consistent with ROS playing a role, but not being solely responsible for, toxicity observed with **8** (Figure S26).

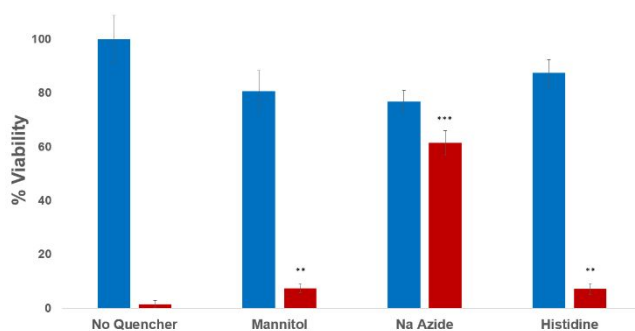


Figure 2. Cell viabilities determined after 4 h by MTT upon pretreatment with ROS scavengers (50 mM) NaN₃, mannitol, or histidine for 2 h, followed by vehicle (blue) or **8** (red, 10 μM) and light (t = 15 min, λ_{irr} = 460–470 nm) Data are averages of three independent experiments, error bars are standard deviations. *** p<0.01 Relating no quencher **8** dosed sample with Na Azide **8** dosed sample. ** p<0.05 Relating no quencher **8** dosed sample with mannitol or histidine **8** dosed sample.

Generation of ¹O₂ was further corroborated with the probe 1,2-diphenylisobenzofuran (DPBF). Rates of ¹O₂ generation relative to methylene blue were determined for compounds **4** and **6–9** under broad band irradiation (λ_{irr} = 500–750 nm) in isopropanol (Table 3).⁵⁰ Wavelengths of light irradiation < 500 nm were excluded using a long pass filter to minimize autooxidation of DPBF that occurs in the absence of photosensitizer. As judged by DPBF depletion, alcohol **4**, a photoproduct derived from **6** and **8**, shows the highest rate of ¹O₂ generation

1 in the series, over double the rate of the efficient photosensitizer methylene blue (Entry 1). The rate of $^1\text{O}_2$
2 generation for **8** was roughly 1.5 times that of methylene blue (Entry 4), whereas the rate for **7** was roughly
3 three times slower than methylene blue (Entry 3). Interestingly, the relative rate for Et derivative **9** (Entry 5)
4 was over 25 times slower than **8**, even though both compounds contain alkyl substituents as X. Acetoxy
5 Me_2BODIPY derivative **6**, which releases acetate upon photolysis,⁴⁴ generates $^1\text{O}_2$ at a rate roughly half that
6 of **8** (Entry 2), suggesting that methyl groups provide optimal levels of $^1\text{O}_2$ generation. Collectively, these data
7 confirm that levels of $^1\text{O}_2$ generation can be tuned over two orders of magnitude by changing the substituent
8 X bound directly to boron. Probably, the methyl groups on boron accelerate intersystem crossing to the triplet
9 excited state, leading to singlet oxygen generation. This idea is consistent with improved photorelease quantum
10 yields for these compounds, since triplet excited states live longer than singlet excited states, providing an
11 extended time window for the photocage to undergo photorelease. Furthermore, data for **6** and **8** reveal that
12 generation of $^1\text{O}_2$ is not the only factor that contributes to cytotoxicity. The caged CTSB inhibitor **8** is >20
13 times more potent than **6** alone or in combination with **2** under light conditions at 4 h. Given that **8** shows a
14 rapid acceleration of CTSB inactivation under light vs. dark conditions (Table 1, Entry 4) and **6** does not (Table
15 1, Entry 2), the rate of CTSB inactivation may contribute to the observed cytotoxicity.
16
17
18
19
20
21
22
23
24
25
26
27
28
29
30
31
32
33
34
35
36
37
38
39
40
41
42
43
44
45
46
47
48
49
50
51
52
53
54
55
56
57
58
59
60

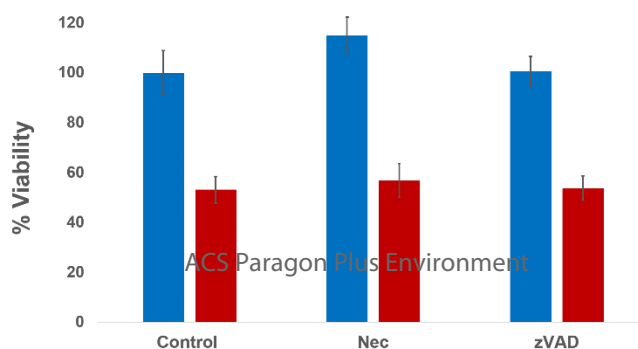
Table 3. Rates of singlet oxygen generation, reported as percentages, relative to methylene blue determined by 1,2-diphenylisobenzofuran (DPBF) depletion ^[a]

Entry	Compound	Relative Rate of DPBF Degradation (%) ^[b]
1	4	202 ± 5
2	6	69 ± 18
3	7	31.3 ± 8.8
4	8	153 ± 35
5	9	6.3 ± 3.8

[a] DPBF absorbance at 410 nm was observed every 30 s of irradiation ($\lambda_{irr} > 500$ nm) time over a 4 min time period for methylene blue and compounds 4 and 6–9. [b] Rates of DPBF degradation by compound 4, 6, 7, 8, or 9 are reported as percentages relative to methylene blue (100%). Data are average of three independent experiments, errors are standard deviations.

Intrigued by findings from the EC₅₀ determinations, we sought to gain a better understanding of how compound 8 elicits its toxic effect in MDA-MB-231 cells. PCR studies were carried out to look for changes in expression of any genetic markers that could be indicative of the nature of the death response. Glucose transporter 1, hexokinase 2, lactose dehydrogenase A, and pyruvate dehydrogenase kinase 1, genes involved in energy metabolism⁵¹ were examined; however, no significant changes in mRNA levels of these markers were observed (data not shown). This finding suggests that the combination of 8 and light does not target energy metabolism directly.

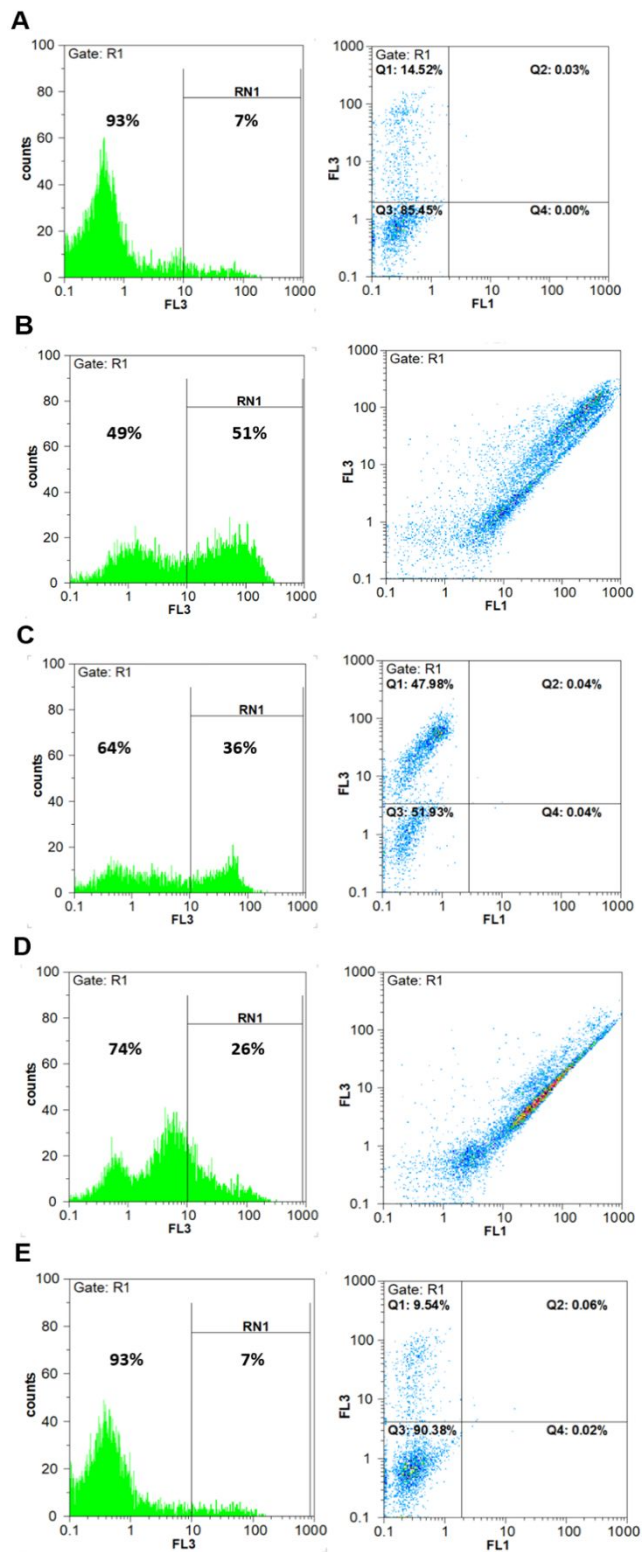
Agents that induce apoptosis usually show little to no cell death at early time points (< 24 h), whereas compounds that induce necrosis often display toxicity shortly after treatment.⁵² To probe the mechanism of



1 cell death, inhibitors of apoptosis and necroptosis were examined. Pretreatment of MDA-MB-231 cells for 2 h
2
3
4 with the RIP-1 kinase inhibitor necrostatin-1 (50 μ M) or the pan-caspase inhibitor Z-VAD-fmk-OMe (20 μ M)
5
6 did not provide significant levels of rescue for cells treated with **8** (2.5 μ M) and light ($t = 15$ min, $\lambda_{\text{irr}} = 460$ -
7
8 470 nm) after 4 h (Figure 3). These data suggest that apoptosis and necroptosis do not play major roles in cell
9
10 death. Consistent with this idea, Western blot analysis also indicated that the executioner enzyme caspase-3
11
12 was not activated at 4 h, indicating that the apoptotic cascade was not operational (Figure S32)
13
14
15
16
17
18
19
20

21 **Figure 3.** Cell viabilities determined after 4 h by MTT upon pretreatment with RIP-1 kinase inhibitor
22 necrostatin-1 (Nec, 50 μ M) or pan-caspase inhibitor Z-VAD-fmk-OMe (zVAD, 20 μ M) for 2 h, followed by
23
24 vehicle (blue) or **8** (red, 2.5 μ M) and light ($t = 15$ min, $\lambda_{\text{irr}} = 460$ –470 nm). Data are representative of three
25
26 independent experiments and are average of quadruplicate wells with error bars as standard deviations.
27
28
29
30
31
32
33
34
35
36
37
38
39
40
41
42
43
44
45
46
47
48
49
50
51
52
53
54
55
56
57
58
59
60

1
2
3
4
5
6
7
8 As opposed to rescue experiments shown in Figure 2, strong supporting evidence for rapid necrotic cell
9 death was obtained by flow cytometry. Cells treated with **8** (10 μ M) and light ($t = 15$ min, $\lambda_{\text{irr}} = 460\text{--}470$ nm)
10 showed similar levels of uptake of the cell impermeable dye 7-aminoactinomycin D (7-AAD) after 4 h to cells
11 treated with H_2O_2 (500 mM), a known inducer of necrosis.⁵² Uptake of 7-AAD is consistent with the loss of
12 the plasma membrane integrity that occurs during rapid necrotic death (Figure 4A-E, S24–28). The dye 7-AAD
13 was chosen over propidium iodide to avoid emission overlap with the BODIPY fluorophore of **8** and its
14 photochemical byproducts, whose contribution to cellular fluorescence in the FL1 channel (516-556 nm) is
15 evident in cells treated with **8** (Figure 4B,D), consistent with the cell permeability of **8**. Importantly, cells
16 treated with **8** (10 μ M) in the dark, or with light alone showed minimal 7-AAD uptake (Figure 4D,A).
17
18
19
20
21
22
23
24
25
26
27
28
29
30
31
32
33
34
35
36
37
38
39
40
41
42
43
44
45
46
47
48
49
50
51
52
53
54
55
56
57
58
59
60



1
2
3 **Figure 4.** Flow cytometric analysis of MDA-MB-231 cells after treatment with A) Vehicle alone
4 and light (t = 15 min, $\lambda_{\text{irr}} = 460\text{--}470$ nm), 4 h; B) **8** (10 μM) and light (t = 15 min, $\lambda_{\text{irr}} = 460\text{--}470$
5 nm), 4 h C) H_2O_2 (500 mM), 3 h; D) **8** (10 μM) in the dark. E) Vehicle in the dark. Cells were
6 harvested and stained with the fluorescent DNA stain 7-AAD ($\lambda_{\text{em}} = 647$ nm) which stains
7 permeabilized cells, consistent with necrosis. Fluorescence signals ($\lambda_{\text{ex}} = 488$ nm) detected were
8 FL1 (516–556 nm) and FL3 (665–685 nm). Fluorescence in FL1 channel in Figures 4B and 4D is
9 due to **8** and BODIPY-derived photochemical byproducts. Data are indicative of three independent
10 experiments. See Supporting information for more details.
11
12
13
14
15
16
17
18
19
20
21

22 Taking all of these observations into consideration, it is important to consider why **8** elicits
23 rapid death in MDA-MB-231 cells at low concentrations, whereas the related analogs **2**, **6**, **7** and
24 **9** do not. Importantly, CTSB regulation the proteolytic network that controls cell death occurs on
25 the minute timescale, where **2**, the inhibitor of choice for selective CTSB inactivation, has been
26 proven to be slowly activated by intracellular esterases and not selective.^{22, 23} Esterase cleavage of
27 **2** is likely not rapid enough to generate high intracellular concentrations of **1** needed for CTSB
28 inactivation on short time scales that leads to necrosis. Light-activated inhibitor **8** combines the
29 ideal properties of **2**, which is cell permeable but not selective, with **1**, which is impermeable but
30 highly selective. The combination of cell permeability, high rate acceleration and selectivity for
31 CTSB inactivation under light vs. in the dark makes **8** and its derivatives promising chemical tools
32 to dissect proteolytic networks of cell survival and death that occur on short time scales. Further
33 photochemical investigations will be needed to understand how the substituent X bound to boron
34 controls the efficiency of uncaging for **8** and its derivatives. Based on the tunable reactivity of
35 BODIPY-protected esters for photorelease and ROS generation demonstrated in this manuscript,
36
37
38
39
40
41
42
43
44
45
46
47
48
49
50
51
52
53
54
55
56
57
58
59
60

1
2
3 we expect to be able to identify compounds that undergo fast photorelease of biologically active
4
5 carboxylic acids with minimal ROS generation that would serve as good chemical tools.
6
7

8 In addition to its rapid inactivation of CTSB, BODIPY-caged inhibitor **8** generates $^1\text{O}_2$.
9
10 Importantly, our data confirm that **8** generates $^1\text{O}_2$ generation more efficiently than methylene
11
12 blue, and that generated $^1\text{O}_2$ contributes to cancer cell death. However, control experiments with
13
14 **2** and **6** vs. **8** suggest that generation of $^1\text{O}_2$ is not the only factor that contributes to cell death.
15
16 Rapid CTSB inactivation may be necessary to steer cells away from apoptosis towards necrotic
17
18 death. The combination of rapid CTSB inactivation with ROS generation is synergistic and may
19
20 be a promising strategy to achieve necrotic cell death *in vivo*. Due to a myriad of problems
21
22 associated with agents that cause apoptosis in the clinic, including positive selection for resistant
23
24 cancer cells during treatment, there has been a resurgence in the interest of agents that cause death
25
26 by means other than apoptosis.
27
28
29
30

31 32 **Conclusion** 33 34 35 36

37 In conclusion, we report the synthesis, photochemical and biological characterization of a series
38
39 of BODIPY-caged CTSB inhibitors. Our data confirm that the photochemical and biological
40
41 properties of these caged inhibitors are highly tunable based on the substituent X bound directly
42
43 to boron. Collectively, this study confirms that the combination of rapid and selective inactivation
44
45 of CTSB with $^1\text{O}_2$ generation achieved with **8** leads to a synergistic effect that steers cancer cells
46
47 away from apoptotic death, favoring necrosis. Further studies to understand the chemistry of **8** and
48
49 its analogs, their use as chemical tools to dissect proteolytic networks of cell survival and death,
50
51 as well as the development of light-activated therapeutics based on this strategy are currently
52
53 underway in our laboratories.
54
55
56
57
58
59
60

Acknowledgments

We gratefully acknowledge the National Institutes of Health (EB 016072), National Science Foundation (CHE 1800395, CHE 1764235) and Wayne State University for support of this research. For instrumentation support we thank the Hütteman laboratory, NSF (0840413) and Penrose Therapeut_x

Supporting Information Available: This material is available free of charge via the Internet.

Synthetic procedures for preparation of 8–10 and characterization data including spectra; procedures and experimental data for quantum yields, rates of ¹O₂ generation, enzyme inactivation, cell viability experiments, Western blot, PCR and flow cytometric analysis

References

- (1) Riese, R. J., and Chapman, H. A. (2000) Cathepsins and compartmentalization in antigen presentation, *Current Op. Immun.* 12, 107-113.
- (2) Foghsgaard, L., Wissing, D., Mauch, D., Lademann, U., Bastholm, L., Boes, M., Elling, F., Leist, M. Jaattela, M. (2001) Cathepsin B Acts as a Dominant Execution Protease in Tumor Cell Apoptosis Induced by Tumor Necrosis Factor, *J. Cell Biol.* 153, 999-1010.
- (3) Araujo, T. F., Cordeiro, A. V., Vasconcelos, D. A. A., Vitzel, K. F., and Silva, V. R. R. (2018) The role of cathepsin B in autophagy during obesity: A systematic review, *Life Sci.* 209, 274-281.
- (4) Muniyappa, R., and Sowers, J. R. (2014) Glycogen synthase kinase-3 β and cathepsin B in diabetic endothelial progenitor cell dysfunction: an old player finds a new partner, *Diabetes* 63, 1194-1197.
- (5) Feldstein, A. E., Werneburg, N. W., Canbay, A., Guicciardi, M. E., Bronk, S. F., Rydzewski, R., Burgart, L. J., and Gores, G. J. (2004) Free fatty acids promote hepatic lipotoxicity by stimulating TNF- α expression via a lysosomal pathway, *Hepatology* 40, 185-194.
- (6) Van Acker, G. J. D., Saluja, A. K., Bhagat, L., Singh, V. P., Song, A. M., and Steer, M. L. (2002) Cathepsin B inhibition prevents trypsinogen activation and reduces pancreatitis severity, *Am. J. Physiol.* 283, G794-G800.
- (7) Aggarwal, N., and Sloane, B. F. (2014) Cathepsin B: Multiple roles in cancer, *Proteomics: Clin. Appl.* 8, 427-437.

- 1
- 2
- 3
- 4 (8) Olson, O. C., and Joyce, J. A. (2015) Cysteine cathepsin proteases: regulators of cancer
- 5 progression and therapeutic response, *Nat. Rev. Cancer* *15*, 712-729.
- 6 (9) Lampe, C. M., and Gondi, C. S. (2014) Cathepsin B inhibitors for targeted cancer therapy, *J.*
- 7 *Cancer Sci. Ther.* *6*, 417-421.
- 8 (10) Turk, B. (2006) Targeting proteases: successes, failures and future prospects, *Nature Rev.*
- 9 *Drug Discov.* *5*, 785-799.
- 10 (11) Kos, J., Mitrovic, A., and Mirkovic, B. (2014) The current stage of cathepsin B inhibitors as
- 11 potential anticancer agents, *Future Med. Chem.* *6*, 1355-1371.
- 12 (12) Katunuma, N. (2011) Structure-based development of specific inhibitors for individual
- 13 cathepsins and their medical applications, *P. Jpn. Acad. B-Phys.* *87*, 29-39.
- 14 (13) Sadaghiani, A. M., Verhelst, S. H. L., Gocheva, V., Hill, K., Majerova, E., Stinson, S.,
- 15 Joyce, J. A., and Bogyo, M. (2007) Design, Synthesis, and Evaluation of In Vivo Potency
- 16 and Selectivity of Epoxysuccinyl-Based Inhibitors of Papain-Family Cysteine Proteases,
- 17 *Chem. Biol.* *14*, 499-511.
- 18 (14) Murata, M., Miyashita, S., Yokoo, C., Tamai, M., Hanada, K., Hatayama, K., Towatari, T.,
- 19 Nikawa, T., and Katunuma, N. (1991) Novel epoxysuccinyl peptides. Selective inhibitors
- 20 of cathepsin B, in vitro, *FEBS Lett.* *280*, 307-310.
- 21 (15) Buttle, D. J., Murata, M., Knight, C. G., and Barrett, A. J. (1992) CA074 methyl ester: a
- 22 proinhibitor for intracellular cathepsin B, *Arch. Biochem. Biophys.* *299*, 377-380.
- 23 (16) Bian, B., Mongrain, S., Cagnol, S., Langlois, M.-J., Boulanger, J., Bernatchez, G., Carrier,
- 24 J. C., Boudreau, F., and Rivard, N. (2016) Cathepsin B promotes colorectal
- 25 tumorigenesis, cell invasion, and metastasis, *Mol. Carcinogen.* *55*, 671-687.
- 26 (17) Satoh, T., Kambe, N., and Matsue, H. (2013) NLRP3 activation induces ASC-dependent
- 27 programmed necrotic cell death, which leads to neutrophilic inflammation, *Cell Death*
- 28 *Dis.* *4*, e644.
- 29 (18) Victor, B. C., Anbalagan, A., Mohamed, M. M., Sloane, B. F., and Cavallo-Medved, D.
- 30 (2011) Inhibition of cathepsin B activity attenuates extracellular matrix degradation and
- 31 inflammatory breast cancer invasion, *Breast Cancer Res.* *13*, R115.
- 32 (19) Ha, S.-D., Martins, A., Khazaie, K., Han, J., Chan, B. M. C., and Kim, S. O. (2008)
- 33 Cathepsin B Is Involved in the Trafficking of TNF- α -Containing Vesicles to the Plasma
- 34 Membrane in Macrophages, *J. Immunol.* *181*, 690-697.
- 35 (20) Balaji, K. N., Schaschke, N., Machleidt, W., Catalfamo, M., and Henkart, P. A. (2002)
- 36 Surface cathepsin B protects cytotoxic lymphocytes from self-destruction after
- 37 degranulation, *J. Exp. Med.* *196*, 493-503.
- 38 (21) Everts, V., Delaisse, J.-M., Korper, W., and Beertsen, W. (1998) Cysteine proteinases and
- 39 matrix metalloproteinases play distinct roles in the subosteoclastic resorption zone, *J. of*
- 40 *Bone Min. Res.* *13*, 1420-1430.
- 41 (22) Bogyo, M., Verhelst, S., Bellingard-Dubouchaud, V., Toba, S., and Greenbaum, D. (2000)
- 42 Selective targeting of lysosomal cysteine proteases with radiolabeled electrophilic
- 43 substrate analogs, *Chem. Biol.* *7*, 27-38.
- 44 (23) Montaser, M., Lalmanach, G., and Mach, L. (2002) CA-074, but not its methyl ester CA-
- 45 074Me, is a selective inhibitor of cathepsin B within living cells, *Biol. Chem.* *383*, 1305-
- 46 1308.
- 47 (24) Steverding, D. (2011) The cathepsin B-selective inhibitors CA-074 and CA-074Me
- 48 inactivate cathepsin L under reducing conditions, *Open Enzyme Inhib. J.* *4*, 11-16.
- 49
- 50
- 51
- 52
- 53
- 54
- 55
- 56
- 57
- 58
- 59
- 60

- 1
2
3 (25) Reich, M., Wiczerzak, E., Jankowska, E., Palesch, D., Boehm, B. O., and Burster, T.
4 (2009) Specific cathepsin B inhibitor is cell-permeable and activates presentation of TTC
5 in primary human dendritic cells, *Immunol. Lett.* *123*, 155-159.
6
7 (26) Stern, I., Schaschke, N., Moroder, L., and Turk, D. (2004) Crystal structure of NS-134 in
8 complex with bovine cathepsin B: a two-headed epoxysuccinyl inhibitor extends along
9 the entire active-site cleft, *Biochem. J.* *381*, 511-517.
10
11 (27) Frizler, M., Stirnberg, M., Sisay, M. T., and Guetschow, M. (2010) Development of nitrile-
12 based peptidic inhibitors of cysteine cathepsins, *Curr. Top. Med. Chem.* *10*, 294-322.
13
14 (28) Devetzi, M., Scorilas, A., Tsiambas, E., Sameni, M., Fotiou, S., Sloane, B. F., and Talieri,
15 M. (2009) Cathepsin B protein levels in endometrial cancer: Potential value as a tumour
16 biomarker, *Gynecol. Oncol.* *112*, 531-536.
17
18 (29) Wang, H., Udukala, D. N., Samarakoon, T. N., Basel, M. T., Kalita, M., Abayaweera, G.,
19 Manawadu, H., Malalasekera, A., Robinson, C., Villanueva, D., Maynez, P., Bossmann,
20 L., Riedy, E., Barriga, J., Wang, N., Li, P., Higgins, D. A., Zhu, G., Troyer, D. L., and
21 Bossmann, S. H. (2014) Nanoplatforms for highly sensitive fluorescence detection of
22 cancer-related proteases, *Photochem. Photobiol. Sci.* *13*, 231-240.
23
24 (30) Rothberg, J. M., Bailey, K. M., Wojtkowiak, J. W., Ben-Nun, Y., Bogyo, M., Weber, E.,
25 Moin, K., Blum, G., Mattingly, R. R., Gillies, R. J., and Sloane, B. F. (2013) Acid-
26 mediated tumor proteolysis: contribution of cysteine cathepsins, *Neoplasia* *15*, 1125-
27 1137.
28
29 (31) Roshy, S., Sloane, B. F., and Moin, K. (2003) Pericellular cathepsin B and malignant
30 progression, *Cancer Metastasis Rev.* *22*, 271-286.
31
32 (32) Szpaderska, A. M., and Frankfater, A. (2001) An intracellular form of cathepsin B
33 contributes to invasiveness in cancer, *Cancer Res.* *61*, 3493-3500.
34
35 (33) Shree, T., Olson, O. C., Elie, B. T., Kester, J. C., Garfall, A. L., Simpson, K., Bell-
36 McGuinn, K. M., Zabor, E. C., Brogi, E., and Joyce, J. A. (2011) Macrophages and
37 cathepsin proteases blunt chemotherapeutic response in breast cancer, *Gene Dev.* *25*,
38 2465-2479.
39
40 (34) Mikhaylov, G., Klimpel, D., Schaschke, N., Mikac, U., Vizovisek, M., Fonovic, M., Turk,
41 V., Turk, B., and Vasiljeva, O. (2014) Selective Targeting of Tumor and Stromal Cells
42 By a Nanocarrier System Displaying Lipidated Cathepsin B Inhibitor, *Angew. Chem., Int.*
43 *Ed.* *53*, 10077-10081.
44
45 (35) Cree, I. A., and Charlton, P. (2017) Molecular chess? Hallmarks of anti-cancer drug
46 resistance, *BMC Cancer* *17*, 10/11-10/18.
47
48 (36) Su, Z., Yang, Z., Xu, Y., Chen, Y., and Yu, Q. (2015) Apoptosis, autophagy, necroptosis,
49 and cancer metastasis, *Mol. Cancer* *14*, 1-14.
50
51 (37) Su, Z., Yang, Z., Xie, L., DeWitt, J. P., and Chen, Y. (2016) Cancer therapy in the
52 necroptosis era, *Cell Death Differ.* *23*, 748-756.
53
54 (38) Jacobson, L. S., Lima, H., Jr., Goldberg, M. F., Gocheva, V., Tsiperson, V., Sutterwala, F.
55 S., Joyce, J. A., Gapp, B. V., Blumen, V. A., Chandran, K., Brummelkamp, T. R., Diaz-
56 Griffero, F., and Brojatsch, J. (2013) Cathepsin-mediated Necrosis Controls the Adaptive
57 Immune Response by Th2 (T helper type 2)-associated Adjuvants, *J. Biol. Chem.* *288*,
58 7481-7491.
59
60 (39) Castano, A. P., Mroz, P., and Hamblin, M.R. (2006) Photodynamic therapy and anti-tumour
immunity, *Nat. Rev. Cancer* *6*, 535-545.

- 1
2
3 (40) de Castro, M. A. G., Bunt, G., and Wouters, F. S. (2016) Cathepsin B launches an apoptotic
4 exit effort upon cell death-associated disruption of lysosomes, *Cell Death Discov.* 2,
5 16012.
6
7 (41) Wouters, F. S., and Bunt, G. (2016) Cathepsin B pulls the emergency brake on cellular
8 necrosis, *Cell Death Dis.* 7, e2170.
9
10 (42) Peterson, J. A., Wijesooriya, C., Gehrman, E. J., Mahoney, K. M., Goswami, P. P.,
11 Albright, T. R., Syed, A., Dutton, A. S., Smith, E. A., and Winter A. H. (2018) Family of
12 BODIPY Photocages Cleaved by Single Photons of Visible/Near-Infrared Light, *J. Am.*
13 *Chem. Soc.* 140, 7343-7346.
14
15 (43) Goswami, P. P., Syed, A., Beck, C. L., Albright, T. R., Mahoney, K. M., Unash, R., Smith,
16 E. A., and Winter, E. A. (2015) BODIPY-Derived Photoremovable Protecting Groups
17 Unmasked with Green Light, *J. Am. Chem. Soc.* 137, 3783-3786.
18
19 (44) Slanina, T., Shrestha, P., Palao, E., Kand, D., Peterson, J. A., Dutton, A. S., Rubinstein, N.,
20 Weinstain, R., Winter, A. H., and Klan, P. (2017) In Search of the Perfect Photocage:
21 Structure–Reactivity Relationships in meso-Methyl BODIPY Photoremovable Protecting
22 Groups, *J. Am. Chem. Soc.* 139, 15168-15175.
23
24 (45) Kuzmic, P. (1996) Program DYNAFIT for the Analysis of Enzyme Kinetic Data:
25 Application to HIV Proteinase, *Anal. Biochem.* 237, 260-273.
26
27 (46) Powers, J. C., Asgian, J. L., Ekici, O. D., and James, K. E. (2002) Irreversible Inhibitors of
28 Serine, Cysteine, and Threonine Proteases, *Chem. Rev.* 102, 4639-4750.
29
30 (47) Buttle, D. J., Murata, M., Knight, C. G., and Barrett, A. J.. (1992) CA074 methyl ester: A
31 proinhibitor for intracellular cathepsin B, *Arch. Biochem. Biophys* 299, 377-380.
32
33 (48) Kamkaew, A., Lim, S. H., Lee, H. B., Kiew, L. V., Chung, L. Y., and Burgess, K. (2013)
34 BODIPY dyes in photodynamic therapy, *Chem. Soc. Rev.* 42, 77-88.
35
36 (49) Dong, S., Hwang, H.-M., Shi, X., Holloway, L., and Yu, H. (2000) UVA-Induced DNA
37 Single-Strand Cleavage by 1-Hydroxypyrene and Formation of Covalent Adducts
38 between DNA and 1-Hydroxypyrene, *Chem. Res. Toxicol.* 13, 585-593.
39
40 (50) Lim, S. H., Thivierge, C., Nowak-Sliwinska, P., Han, J., van den Bergh, H. Wagnieres, G.
41 Burgess, K., and Lee, H. B. (2010) In Vitro and In Vivo Photocytotoxicity of Boron
42 Dipyrromethene Derivatives for Photodynamic Therapy, *J. Med. Chem.* 53, 2865-2874.
43
44 (51) Tanner, L. B., Goglia, A. G., Wei, M. H., Sehgal, T., Parsons, L. R., Park, J. O., White, E.,
45 Toettcher, J. E., and Rabinowitz, J. D. (2018) Four Key Steps Control Glycolytic Flux in
46 Mammalian Cells, *Cell Systems* 7, 49-62.
47
48 (52) Vanden Berghe, T., Vanlangenakker, N., Parthoens, E., Deckers, W., Devos, M., Festjens,
49 N., Guerin, C.J., Brunk, U. T., Declercq, W., and Vandenabeele, P. (2010) Necroptosis,
50 necrosis and secondary necrosis converge on similar cellular disintegration features, *Cell*
51 *Death Differ.* 17, 922-930.
52
53
54
55
56
57
58
59
60

TOC Graphic

